Acta Crystallographica Section F
Structural Biology and Crystallization Communications
ISSN 1744-3091
Editors: **H. M. Einspahr and M. S. Weiss**

Room-temperature X-ray diffraction studies of cisplatin and carboplatin binding to His15 of HEWL after prolonged chemical exposure

Simon W. M. Tanley, Antoine M. M. Schreurs, Loes M. J. Kroon-Batenburg and John R. Helliwell

Acta Cryst. (2012). F**68**, 1300–1306

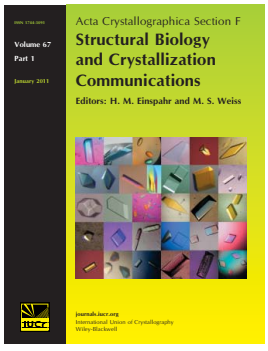

Acta Crystallographica Section F: Structural Biology and Crystallization Communications is a rapid all-electronic journal, which provides a home for short communications on the crystallization and structure of biological macromolecules. Structures determined through structural genomics initiatives or from iterative studies such as those used in the pharmaceutical industry are particularly welcomed. Articles are available online when ready, making publication as fast as possible, and include unlimited free colour illustrations, movies and other enhancements. The editorial process is completely electronic with respect to deposition, submission, refereeing and publication.

Acta Crystallographica Section F
Structural Biology and Crystallization Communications
ISSN 1744-3091

Room-temperature X-ray diffraction studies of cisplatin and carboplatin binding to His15 of HEWL after prolonged chemical exposure

Simon W. M. Tanley,[a] Antoine M. M. Schreurs,[b] Loes M. J. Kroon-Batenburg[b] and John R. Helliwell[a]*

[a]School of Chemistry, Faculty of Engineering and Physical Sciences, University Of Manchester, Brunswick Street, Manchester M13 9PL, England, and [b]Crystal and Structural Chemistry, Bijvoet Center for Biomolecular Research, Faculty of Science, Utrecht University, Padualaan 8, 3584 CH Utrecht, The Netherlands

Correspondence e-mail: john.helliwell@manchester.ac.uk

Received 27 July 2012
Accepted 8 October 2012

PDB References: lysozyme, complexes with cisplatin, 4g49; 4g4a; 4g4b; complexes with carboplatin, 4g4c; 4g4h

The anticancer complexes cisplatin and carboplatin are known to bind to both the N^{δ} and the N^{ε} atoms of His15 of hen egg-white lysozyme (HEWL) in the presence of dimethyl sulfoxide (DMSO). However, neither binds in aqueous media after 4 d of crystallization and crystal growth, suggesting that DMSO facilitates cisplatin/carboplatin binding to the N atoms of His15 by an unknown mechanism. Crystals of HEWL cocrystallized with cisplatin in both aqueous and DMSO media, of HEWL cocrystallized with carboplatin in DMSO medium and of HEWL cocrystallized with cisplatin and *N*-acetylglucosamine (NAG) in DMSO medium were stored for between seven and 15 months. X-ray diffraction studies of these crystals were carried out on a Bruker APEX II home-source diffractometer at room temperature. Room-temperature X-ray diffraction data collection removed the need for cryoprotectants to be used, ruling out any effect that the cryoprotectants might have had on binding to the protein. Both cisplatin and carboplatin still bind to both the N^{δ} and N^{ε} atoms of His15 in DMSO media as expected, but more detail for the cyclobutanedicarboxylate (CBDC) moiety of carboplatin was observed at the N^{ε} binding site. However, two molecules of cisplatin were now observed to be bound to His15 in aqueous conditions. The platinum peak positions were identified using anomalous difference electron-density maps as a cross-check with $F_o - F_c$ OMIT electron-density maps. The occupancies of each binding site were calculated using *SHELXTL*. These results show that over time cisplatin binds to both N atoms of His15 of HEWL in aqueous media, whereas this binding is speeded up in the presence of DMSO. The implication of cisplatin binding to proteins after a prolonged period of time is an important consideration for the length of treatment in patients who are given cisplatin.

1. Introduction

Cisplatin and carboplatin (Supplementary Fig. S1[1]) are platinum anticancer drugs which target DNA. However, 90% of their reported binding is to plasma proteins (Fischer *et al.*, 2008). A variety of different proteins have been studied for their binding affinity to cisplatin using either mass spectrometry or X-ray diffraction, including a copper transporter (Arnesano & Natile, 2008; Crider *et al.*, 2010), a copper chaperone (Boal & Rosenzweig, 2009), superoxide dismutase (Calderone *et al.*, 2006; Casini *et al.*, 2008), cytochrome *c* (Casini *et al.*, 2006; Casini, Gabbiani *et al.*, 2007), human albumin (Ivanov *et al.*, 1998), ubiquitin (Hartinger *et al.*, 2007, glutathione reductase (Zimmermann & Burda, 2010), Na^+/K^+-ATPase (Huličiak *et al.*, 2012) and hen egg-white lysozyme (HEWL; Casini, Mastrobuoni *et al.*, 2007; Tanley *et al.*, 2012). Carboplatin binding affinity, however, has been less studied, with one study using mass spectrometry (Casini, Mastrobuoni *et al.*, 2007) and another study involving X-ray diffraction (Tanley *et al.*, 2012), both of which looked at binding to HEWL. In our preceding paper (Tanley *et al.*, 2012), HEWL was cocrystallized with cisplatin or carboplatin in both aqueous medium and medium with added DMSO, using either glycerol or Paratone as a cryoprotectant, and cisplatin was also cocrystallized with HEWL and a ligand (*N*-acetylglucosamine; NAG)

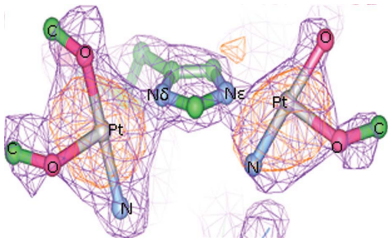

[1] Supplementary material has been deposited in the IUCr electronic archive (Reference: YT5048).

Table 1
X-ray crystallographic data details and protein–ligand model-refinement statistics for all crystals analysed.

Values in parentheses are for the last shell.

	Carboplatin/DMSO	Cisplatin/DMSO	Cisplatin/NAG/DMSO	Cisplatin/aqueous	Carboplatin/DMSO, 100 K
PDB code	4g4c	4g4a	4g4b	4g49	4g4h
Crystal storage time (months)	13	14	7	15	13
Crystal dimension (mm)	0.2	0.25	0.16	0.3	0.25
Data-collection temperature (K)	300	300	300	300	100
Data reduction					
Space group	$P4_32_12$	$P4_32_12$	$P4_32_12$	$P4_32_12$	$P4_32_12$
Unit-cell parameters (Å, °)	$a = b = 79.23$, $c = 37.89$, $\alpha = \beta = \gamma = 90.0$	$a = b = 79.04$, $c = 38.04$, $\alpha = \beta = \gamma = 90.0$	$a = b = 78.82$, $c = 38.02$, $\alpha = \beta = \gamma = 90.0$	$a = b = 78.99$, $c = 37.12$, $\alpha = \beta = \gamma = 90.0$	$a = b = 77.11$, $c = 36.70$, $\alpha = \beta = \gamma = 90.0$
Protein molecular mass (Da)	14700	14700	14700	14700	14700
Molecules per asymmetric unit	1	1	1	1	1
Crystal-to-detector distance (mm)	39.19	39.19	39.19	39.19	40.00
Observed reflections	285065	360972	256686	96714	410176
Unique reflections†	15602	9038	13385	8952	14368
Resolution (Å)	35.43–2.00 (2.03–2.00)	35.35–2.40 (2.44–2.40)	39.41–2.10 (2.13–2.10)	35.18–2.40 (2.44–2.40)	34.52–2.00 (2.04–2.00)
Completeness (%)	99.83 (96.9)	99.9 (100)	99.9 (100)	99.9 (100)	99.9 (100)
$R_{\rm merge}$†	0.157 (0.855)	0.180 (0.947)	0.177 (0.749)	0.151 (0.623)	0.163 (0.657)
$R_{\rm meas}$	0.161 (0.897)	0.182 (0.963)	0.182 (0.779)	0.158 (0.661)	0.166 (0.681)
$\langle I/\sigma(I)\rangle$	18.0 (4.1)	23.6 (6.7)	16.1 (5.1)	13.7 (3.9)	18.5 (4.8)
Multiplicity	18.3 (10.0)	39.9 (30.5)	19.2 (13.2)	10.8 (8.9)	28.6 (13.6)
Cruickshank DPI (Å)	0.13	0.50	0.21	0.56	0.24
Average B factor (Å^2)	19.2	24.8	24.0	35.4	18.0
Refinement					
R factor/$R_{\rm free}$ (%)	16.1/20.3	16.3/21.0	15.9/22.7	17.5/20.9	20.5/26.7
R factor, all (%)	16.3	16.5	16.2	17.7	20.7
R.m.s.d. bonds (Å)/angles (°)	0.018/1.831	0.014/2.399	0.018/2.531	0.012/1.417	0.018/1.799
Ramachandran values (%)					
Most favoured	97.6	96.1	97.6	97.6	96.1
Additional allowed	2.4	3.9	2.4	2.4	3.9
Disallowed	0	0	0	0	0

† Anomalous separate.

(PDB entries 4dd0, 4dd1, 4dd2, 4dd3, 4dd4, 4dd6, 4dd7, 4dd9, 4dda, 4ddb and 4ddc). These results indicated that in the presence of DMSO in the cocrystallization buffer one molecule of cisplatin/carboplatin binds to the N^{δ} and N^{ε} atoms of residue His15, which is the only histidine residue in HEWL. The structural unit of one histidine bound to two platinum centres means that in the imidazole of this histidine the usual N-hydrogen of such a residue is absent and that both N atoms are sp^2-hybridized with nitrogen lone pairs in the plane of the imidazole ring (an imidazolyl anion), providing two N atoms at which a metal centre can bind. The loss of the N-hydrogen is deemed to be made possible by either the chloride or the acetate ions in the crystallization conditions. This result was observed for both cryoprotectants used and also when cisplatin was cocrystallized with NAG. However, in aqueous conditions no platinum binding to His15 was observed, giving rise to the conclusion that DMSO somehow facilitates cisplatin/carboplatin binding to the His15 residue.

This new study focuses on exploring cisplatin/carboplatin binding to both the N^{δ} and N^{ε} atoms of His15 in further detail using the same batch of crystals used for the previous study but after their prolonged storage in their mother liquor and thereby their prolonged chemical exposure to these metal compounds (Tanley *et al.*, 2012). X-ray diffraction data were measured at room temperature (RT), which removed the need for cryoprotectants, decreased the number of data sets collected and removed any effects that glycerol/Paratone or cryocooling would have on the protein. Of the previous 11 crystal types tested, four were used in this study: HEWL cocrystallized with cisplatin in aqueous and DMSO-added media, HEWL cocrystallized with carboplatin in DMSO-added medium and HEWL cocrystallized with cisplatin and NAG in DMSO-added medium. This new set of experiments assesses whether the binding occupancies at each site increase over time, whether extra detail is observed at the binding sites for all four conditions and whether cisplatin aqueous conditions show binding at His15. The fragility of the 'carboplatin/lysozyme/aqueous conditions' crystals unfortunately prevented their crystal mounting and detailed study.

2. Materials and methods

2.1. Materials

Cisplatin, HEWL and NAG were purchased from Sigma–Aldrich, UK. Carboplatin was purchased from Calbiochem, USA, DMSO from Cambridge Isotope Laboratories, UK and sodium chloride (NaCl) from Fisher Scientific, UK. Sodium acetate and acetic acid were purchased from BDH in AnalaR grade.

2.2. Crystallization conditions

The cocrystallization conditions for each crystal at pH 4.7 are the same as those previously published (Tanley *et al.*, 2012), apart from the increased crystal storage time (Table 1) and the use of only 0.66 m*M* DMSO for the cisplatin/DMSO cocrystallization condition compared with the 1 m*M* DMSO previously used. The crystallization conditions were set up to begin with in 5, 7.5 and 10% DMSO media with cisplatin and HEWL. The 7.5% DMSO condition (1 m*M*) was used for the cryo study (Tanley *et al.*, 2012). When trying to use these crystals for the room-temperature study, the crystals could not be detached from their pot, but it was possible to obtain some crystals from the 5% (0.66 m*M*) DMSO condition pot; the platinum occupancy values for the 5 and 7.5% DMSO conditions are very similar (see below and Tanley *et al.*, 2012).

2.3. X-ray data collection, structure solution and refinement

Crystals were mounted in thin-walled 0.7–1.0 mm glass/quartz capillary tubes. The crystals were then centred on a home-source Bruker APEX II CCD detector diffractometer. Data were collected

Table 2
Occupancies (shown as percentages) of cisplatin and carboplatin binding to the N^{δ} and N^{ϵ} atoms of His15 refined using *SHELXTL* and the Pt—N distances (Å) for each binding site.

The precision of these distances are indicated in parentheses based on the Cruickshank DPI (Cruickshank, 1999; corrected for their atomic *B* values *versus* the average *B* value) coordinate errors for each pair of atoms. The precision of the occupancies is approximately ±5% (see Tanley *et al.*, 2012). The table contains all four RT crystals tested and the one new cryo crystal structure, along with the two cryocooled '8 d' crystal structure examples from Tanley *et al.* (2012).

	N^{δ} binding site		N^{ϵ} binding site	
	Occupancy (%)	Pt—N distance (Å)	Occupancy (%)	Pt—N distance (Å)
Cisplatin/aqueous, RT	50	2.4 (1.0)	33	2.2 (1.0)
Cisplatin/DMSO, RT	73	2.0 (0.8)	41	2.5 (0.9)
Cisplatin/DMSO/NAG, RT	69	2.4 (0.4)	47	2.2 (0.4)
Cisplatin/DMSO/glycerol, cryocooled, 8 d	70	2.4 (0.2)	52	2.3 (0.2)
Carboplatin/DMSO, RT	67	2.2 (0.2)	51	2.3 (0.2)
Carboplatin/DMSO, cryocooled, 15 months	68	2.4 (0.4)	47	2.1 (0.4)
Carboplatin/DMSO, cryocooled, 8 d	66	2.3 (0.2)	53	2.3 (0.2)

using an X-ray wavelength of 1.5418 Å at room temperature (RT; 300 K), with the detector set at 39.19 mm from the crystal and with an exposure time of 40 s per 0.5° crystal rotation for all four crystals measured. Supplementary Table 1 summarizes the detector swing angles and the sweeps of data collected for each data set derived from the Bruker data-collection strategy program.

All data sets were processed using *Eval*15 (Schreurs *et al.*, 2010). The capillary approximately, but closely, coincided with the φ axis of the goniostat. During integration, it was realised that for the ω scans for some of the angular range the capillary absorbed diffraction spots, basically when the capillary pointed at the detector face (see video clip deposited as Supplementary Material). Therefore, all reflections with a reflected beam less than 40° from the capillary axis were removed from the data list. [In future, the simpler approach of φ scans should be employed.]

For the carboplatin/DMSO crystals, a data set was also collected at 100 K. A crystal was mounted into a loop using silicone oil as a cryoprotectant. The crystal was then also centred on our home-source Bruker APEX II CCD detector diffractometer. Data were collected using an X-ray wavelength of 1.5418 Å at 100 K, with the detector at 40.00 mm from the crystal. Exposure times were set at either 10 or 30 s per 0.5° crystal rotation. These data were also processed using the *Eval*15 program.

All structures were solved by molecular replacement with *Phaser* (McCoy *et al.*, 2007) and restrained refinement with TLS by *REFMAC*5 (Vagin & Teplyakov, 2010) in *CCP*4*i* (McNicholas *et al.*, 2011) using the reported lysozyme structure (PDB entry 2w1y; Cianci *et al.*, 2008) as a molecular search model. Model building, adjustment and refinement were carried out using the *Coot* molecular-graphics program (Emsley & Cowtan, 2004) and *REFMAC*5 in *CCP*4*i*, respectively. Ligand-binding occupancies were calculated using *SHELXTL* (Sheldrick, 2008). Crystallographic and refinement parameters are summarized in Table 1.

3. Results

3.1. Cisplatin binding to His15

For the three crystals cocrystallized with cisplatin, cisplatin was found to be bound to the N^{δ} atom and the N^{ϵ} atom of the imidazole ring of His15, with the clarity of each of the Cl and N atoms varying in each case (Figs. 1*a*, 1*b* and 1*c*). Comparing the electron density observed in these conditions with that from one of the data sets from our previous cryocooling study (Tanley *et al.*, 2012; Fig. 1*d*) shows no

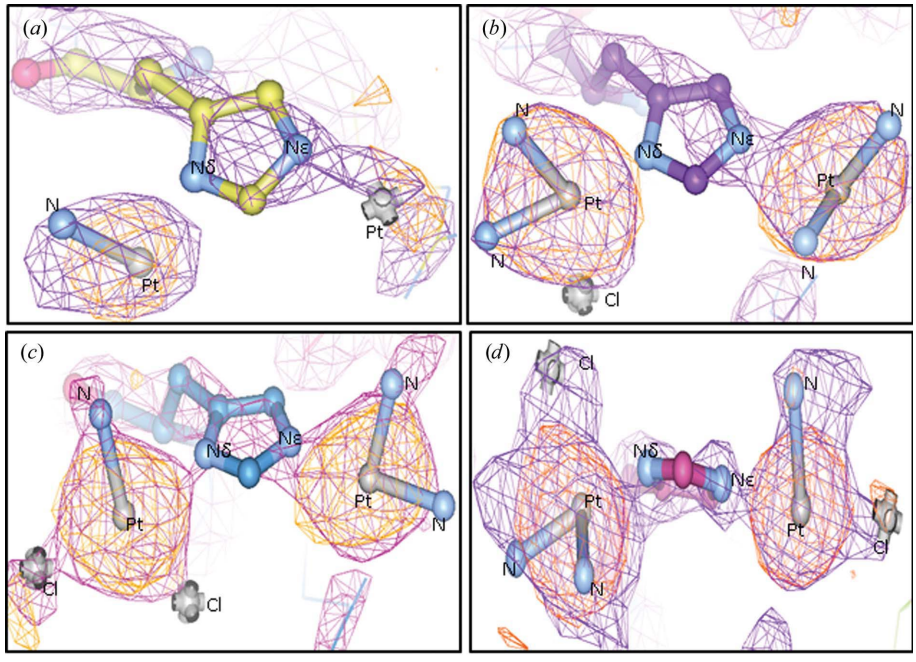

Figure 1
Cisplatin binding to HEWL in aqueous medium with 15 months chemical exposure (*a*), in 5% DMSO medium with 14 months chemical exposure (*b*), and on cocrystallization with 7.5% DMSO and NAG with 7 months chemical exposure (*c*), with data collection in each case at RT. (*d*) Cisplatin in 7.5% DMSO medium with Paratone as the cryoprotectant after 8 d cocrystallization studied at cryo temperatures (Tanley *et al.*, 2012) for comparison. These $F_o - F_c$ OMIT electron-density maps are shown at the 1.5σ level (in purple) and the anomalous difference electron-density maps (in orange) are shown at the 2.5σ level. The atoms bound to each Pt ion differ based on the electron density observed and are labelled, with the N^{δ} binding sites on the left-hand side and the N^{ϵ} binding sites on the right-hand side in each figure. The Pt—N distances and the precisions of these distances are given in Table 2.

real difference in the density observed, although the atoms are placed slightly differently. The exception to this is the cisplatin in aqueous medium experiment (Fig. 1*a*), where we now observe some degree of binding of cisplatin at His15 compared with the absence of binding after 4 d observed in the previous study. For this data set, only one N atom in the N^{δ} binding site can be modelled binding to the Pt ion based on the electron density and only the Pt ion is observed at the N^{ε} binding site. Fig. 1(*c*) does show the unusual characteristic of the N^{δ} atom replacing an amino group, rather than a Cl atom, which acts as a leaving group on cisplatin. Calderone *et al.* (2006) also observed this in their study of cisplatin binding to His19 of cuprozinc superoxide dismutase. In their study, they only observed electron density for the Pt ion and the two Cl atoms, with both of the amino groups being displaced; hence, this displacement of an amino group has been observed previously. The occupancies of the cisplatin molecule at each binding site are given in Table 2 and were calculated using *SHELXTL* (Sheldrick, 2008), with a comparison to the cryo-example from the previous study also being given. All occupancy values are expected to have a standard uncertainty of approximately ±5% (Tanley *et al.*, 2012).

3.2. Carboplatin binding to His15

Carboplatin is also found to be coordinated to both the N^{δ} and N^{ε} atoms of His15 (Fig. 2). Comparing the binding sites in the RT data study after 13 months of prolonged chemical exposure (Fig. 2*a*) with those in one of the cryocooled carboplatin data sets from the previous study after 8 d of cocrystallization (Fig. 2*b*; Tanley *et al.*, 2012) and those in the carboplatin cryocooled data set after 13 months of prolonged chemical exposure (Fig. 2*c*), extra electron density is observed at the N^{ε} binding site in the $F_o - F_c$ OMIT map for the RT case (Fig. 2*a*), which is interpretable as a portion of the cyclobutane-dicarboxylate (CBDC) moiety of carboplatin (Supplementary Fig. S1). This extra electron density is not observed in either of the cryocooled data sets (see §3.3 for more detail). For the N^{δ} binding site, the electron density is very similar for both the RT and cryo-cooled data sets, with both showing evidence for a portion of the CBDC moiety (Fig. 2). The occupancy values for carboplatin binding to both sites were refined using *SHELXTL* (Sheldrick, 2008) and are given in Table 2, along with the Pt—N distances, and with the values for the cryocooled example after 8 d crystallization as a comparison.

3.3. Carboplatin binding to the N^{ε} atom of His15 in more detail

Comparing the $F_o - F_c$ OMIT electron-density map at the N^{ε} binding site (Fig. 2) of the RT 13 months prolonged chemical exposure data set with the cryocooled data set after 8 d crystallization shows a difference, with extra detail being seen in the RT data set. This extra detail corresponds to a downwards shift of the NH1 atom of the Arg14 residue by 0.8 Å (Fig. 3*a*), meaning that there is space for an extra atom to be accommodated. A cryocooled data set after 13 months prolonged chemical exposure was also collected as a comparison with the RT data after 13 months prolonged chemical exposure. This was to confirm whether the extra detail observed was a consequence of the temperature of data collection or was based on the length of time of crystallization and exposure to carboplatin. The cryocooled data set after 13 months showed the same degree of detail of electron density as the cryocooled 8 d crystallization data set (Figs. 2*b* and 2*c*). Comparing the position of the NH1 atom of Arg14 between the RT 13 months data set and the cryocooled 13 months data set, the NH1 atom is shifted both downwards and sideways by 1.8 Å (Fig. 3*b*). To confirm whether these shifts are significant, the coordinate error of each atom can be calculated using (1) based on the Cruickshank DPI values (Table 1; Cruickshank, 1999; Blow, 2002), taking account of the atomic B ($B_{\rm atom}$) *versus* the average B ($B_{\rm average}$),

$$\text{coordinate error of atom} = \text{DPI} \times (B_{\rm atom}/B_{\rm average})^{1/2}. \quad (1)$$

The standard deviation of the calculated shift is determined using the coordinate error of the NH1 atom of the Arg14 residue in both structures (1 and 2),

$$\text{standard deviation} = [(\text{coordinate error 1})^2 + (\text{coordinate error 2})^2]^{1/2}. \quad (2)$$

The value and standard uncertainty for the shift between the cryo-cooled 13 months data set and the RT 13 months data set is 1.8 ± 0.4 Å and the value and standard uncertainty of the shift between the RT 13 months data set and the cryocooled 8 d data set is 0.8 ± 0.2 Å. Thus, the shift of the NH1 atom of Arg14 is significant in both cases and can thus explain the extra detail in the $F_o - F_c$ OMIT electron-density map around the N^{ε} binding site that is observed in the RT 13 months prolonged chemical exposure cocrystallization data set.

4. Discussion

4.1. The initial experimental concepts for these studies

The interest in embarking on this study was to explore in further detail the binding of cisplatin and carboplatin to His15 of HEWL in both DMSO and aqueous media but after a prolonged period of chemical exposure. In our previous study (Tanley *et al.*, 2012), experiments involving HEWL cocrystallization with cisplatin and carboplatin were undertaken with crystal-growth times of between 4

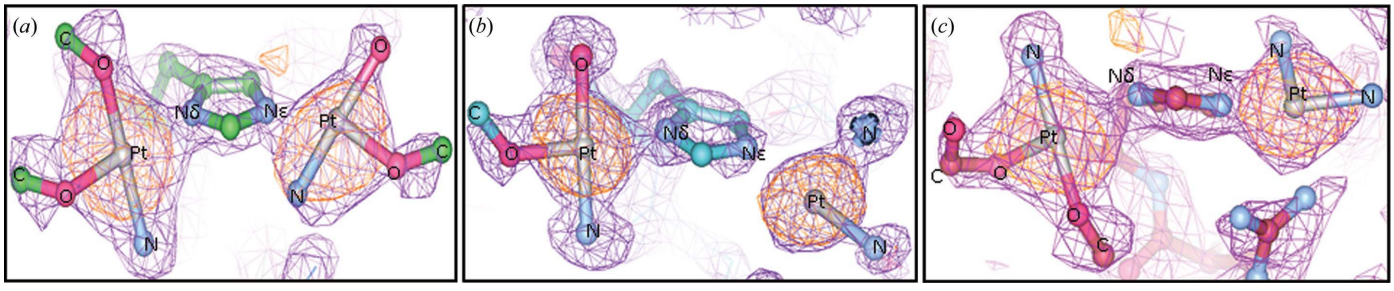

Figure 2
Carboplatin binding to His15. (*a*) RT data set for carboplatin binding to HEWL in 7.5% DMSO medium after 13 months of crystal growth, (*b*) cryocooled data set for carboplatin binding to HEWL in 7.5% DMSO media with Paratone as the cryoprotectant after 8 d cocrystallization (from Tanley *et al.*, 2012) and (*c*) cryocooled data set for carboplatin binding to HEWL in 7.5% DMSO media with silicone oil as the cryoprotectant after 13 months of crystal growth. The $F_o - F_c$ OMIT electron-density maps (in purple) are shown at 1.5σ and the anomalous difference electron-density maps (in orange) are shown at 3σ. The atoms of the carboplatin molecule are labelled, along with the N^{δ} and N^{ε} atoms of His15.

and 8 d. These results showed that the addition of DMSO facilitated the binding of these Pt complexes to both the N^{δ} and N^{ε} atoms of His15, with high-occupancy binding being observed for both binding sites (~65% for N^{δ} and ~50% for N^{ε}), whereas in aqueous conditions this binding was not observed.

This new study used four of the previously grown crystal types which had been left on the shelf for between seven and 15 months. HEWL cocrystallized with carboplatin in aqueous medium was not studied here owing to the fragility of the crystals, which prevented their mounting in a capillary. RT X-ray diffraction was used as this removed the need for cryoprotectants: the previous study showed that both glycerol and Paratone can bind to the protein. The use of RT also had the practical benefit of reducing the number of X-ray diffraction data sets needed.

4.2. Cisplatin/carboplatin binding to His15 in further detail

Cisplatin binding in this study shows many similarities compared with the previous study (Fig. 1), although the atoms discerned to be bound to the Pt ion do vary somewhat from data set to data set. The occupancy values for the platinum binding to both the N^{δ} atom (69–73%) and the N^{ε} atom (41–47%) are comparable to those observed in the previous study (~65% ± 5% for the N^{δ} binding site and ~50% ± 5% for the N^{ε} binding site), with the exception of the cisplatin aqueous data set, which will be discussed in more detail below (§4.3).

Looking at carboplatin binding to the N^{ε} binding site, there is a difference between this study and the previous results after only 8 d of crystal growth, as only the two N atoms of the complex were observed. Now, however, we can see evidence for a portion of the CBDC moiety and for one N atom bound to the Pt ion (Fig. 2*a*). In comparing the N^{ε} binding sites in the RT 13 months prolonged chemical exposure study and the cryocooled data set after 8 d crystallization (Fig. 3*a*), it was noted above that the NH1 atom of Arg14 had shifted downwards by 0.8 Å. Also, the Arg14 NH1 atom had shifted to the left and downwards by 1.8 Å compared with the cryocooled data set after 13 months prolonged chemical exposure (Fig. 3*b*). These shifts are significant (0.8 ± 0.2 and 1.8 ± 0.4 Å) based on the standard deviations of the coordinate error for the NH1 atom in both structures using (1) and (2). This significant atomic shift observed in the RT data set corresponds to being able to observe extra detail in the $F_o - F_c$ OMIT electron-density map around the N^{ε} binding site, and thus extra atoms can be modelled into the electron density (Fig. 2). The Arg14 residue does not shift downwards between the two cryocooled data sets; it has only shifted sideways, meaning that both the cryocooled data sets have similar electron density and only the Pt ion and two N atoms can be modelled (Fig. 2*b* and 2*c*).

At RT we observe that Arg14 moves out of the way, leading to more detail being observed in the electron-density maps at the N^{ε} binding site. This must have taken place in the cryocooled crystals because all the crystals were cocrystallized at RT; it appears that on cryocooling the crystal becomes disordered or the Arg14 residue is frozen in a different conformation, therefore obscuring details in the electron-density maps. Hence, collecting the data at RT has resulted in more detail being observed at the N^{ε} binding site owing to the conformation of the Arg14 residue not being affected by the data-collection temperature, as was the case in the 100 K structure. The resolution of the RT 13 months prolonged chemical exposure data set extended to 2.0 Å, the 13 months prolonged chemical exposure cryocooled data set extended to 2.08 Å resolution (Table 1) and the 8 d cryocooled data set extended to 1.6 Å resolution (Tanley *et al.*, 2012). Thus, diffraction resolution is not the reason why more detail was observed at RT, as the two cryocooled data sets show very similar electron density at the N^{ε} binding site (Fig. 2) even with these different resolution limits. Another possibility is that the observation of extra detail after 13 months of prolonged chemical exposure could arise from a change in pH over time. However, measuring the pH of each crystallization pot resulted in the same pH being observed (pH 4.7), except for cisplatin in 5% DMSO, which had a pH of 5.0. Also, as the occupancy values and the electron-density maps of cisplatin binding to His15 were very similar for both the short and prolonged chemical exposures, a change in pH can be ruled out as the reason for the observation of extra detail.

We should also consider the possibility of relatively poor solubility, as cisplatin is known to have a low solubility of 0.25 mg ml^{-1} in water and of 1 mg ml^{-1} in 0.9% NaCl. The conditions used here were 3 mg ml^{-1} cisplatin for all cases apart from the cisplatin with NAG cocrystallization, where cisplatin was used at 1.1 mg ml^{-1}, but this is still a threefold molar excess over the protein. A 1 mg ml^{-1} solution of cisplatin equates to a molar concentration of 3.3 m*M*, which is the same molar concentration as that of HEWL in all conditions apart

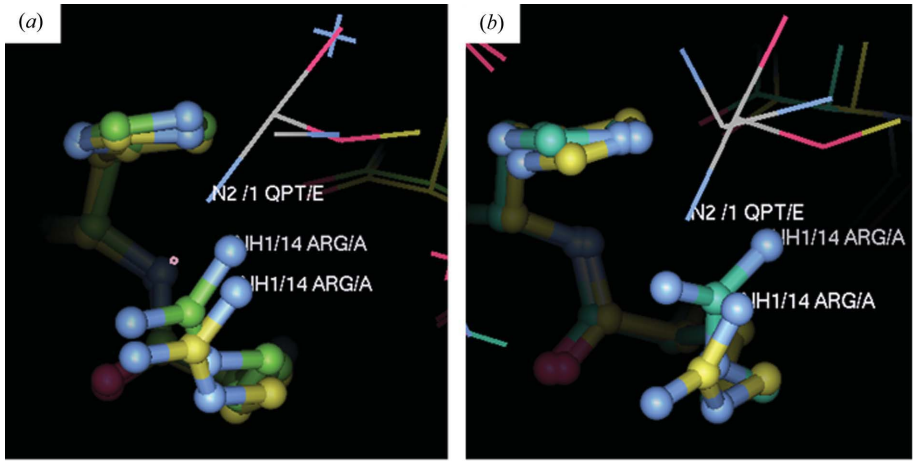

Figure 3
Shift of the Arg14 residue. (*a*) Comparison between the RT 13 months prolonged chemical exposure data set (yellow) and the 8 d cryocooled data set (green), with the downwards shift of the NH1 atom being 0.8 Å. (*b*) Comparison of the RT 13 months crystal storage data set (yellow) with the cryocooled 13 months crystal storage data set (blue), with a downwards and left-hand shift of the NH1 atom by 1.8 Å. The shift of the RT 13 months crystal storage data set Arg 14 residue is sufficient to allow extra detail to be observed in the N^{ε} binding site. This is shown by the N2 atom of the carboplatin molecule (QPT) from the RT 13 months data set; this atom now has space that was not present in both the cryocooled data sets.

from the cocrystallization of cisplatin with NAG. Hence, if only 1 mg of cisplatin was soluble to start with, and the increased chemical exposure caused more cisplatin/carboplatin to dissolve, this could cause the extra detail that was observed compared with 8 d of crystallization and also increased occupancy values. However, we do not observe an increase in occupancy after prolonged chemical exposure, with the exception of the cisplatin aqueous crystallization conditions, which are described in more detail in §4.3. The other crystallizations must have already reached saturation after 8 d of crystallization.

Overall, the temperature of data collection in this study has led to differences being observed in the electron-density maps, with those at RT showing extra detail compared with those at 100 K for the N^{ε} binding site.

In the N^{δ} binding site (Fig. 2), the OMIT electron-density map detail is comparable between the studies. However, the greater detail observed at the N^{ε} binding site in the RT data led us to model in a portion of the CBDC moiety into the N^{δ} binding sites of the cryocooled data. Again, like cisplatin, the carboplatin Pt occupancies in this study are comparable to the previous results (67% and 51% for the N^{δ} and N^{ε} binding sites, respectively, compared with 66% and 53% for the cryocooled data), meaning that the system had reached chemical equilibrium.

Comparing the RT structures with those of their 100 K counterparts using *LSQKAB* in *CCP*4*i* and plotting the r.m.s. differences between the structures shows some significant changes (Supplementary Table S2). Comparisons made were for carboplatin/DMSO (Supplementary Fig. S2 comparing the RT 13 months prolonged chemical exposure case with the 100 K 13 months prolonged chemical exposure case; Supplementary Fig. S3 compares the RT 13 months prolonged chemical exposure case with the 100 K 8 d crystallization case), cisplatin/DMSO (Supplementary Fig. S4), cisplatin/aqueous (Supplementary Fig. S5) and cisplatin/NAG/DMSO (Supplementary Fig. S6). Each supplementary figure shows the r.m.s. differences between the structures and the average *B* factors per residue for each structure. The plots of the *B* factors for each pair of structures shows the same overall trend, with the RT data sets having higher *B* factors overall, as expected. The significant changes in the r.m.s. difference plots occur at Gly71 in all comparisons; however, there are also some other significant changes which are given in Supplementary Table S2. All of the residues that show these significant changes between the 100 K and RT structures are parts of loop regions in HEWL. To our knowledge, these regions of HEWL are not chemically significant and also are not likely to be involved in the differences observed owing to the extra detail at the N^{ε} binding site.

RT data collection, of course, has the disadvantage of potentially increased X-ray radiation damage compared with data collection at 100 K. No radiation damage was observed in our data sets, but the $R_{\rm merge}$ values (Table 1) for each crystal are high, which is a possible sign of radiation damage. The main reason for this, however, was significant data-scaling problems, most likely because the crystals did not sit completely still in their capillary. Additionally, the RT crystals do not diffract to a very high resolution, so that low $R_{\rm merge}$ values would not be expected. Also, whilst the apparatus is very good the X-ray source is not a rotating anode and thus the X-ray beam intensity is weaker than what would be considered the usual norms for, for example, synchrotron data.

Another concern could be chemically specific radiation damage, which we now discuss. For example, Ramagopal *et al.* (2005) showed that protein–heavy atom bonds can be severely affected by X-ray radiation damage; thus, not taking the radiation-damage effect into account could cause a problem in the occupancy values of heavy-metal atoms or metal-containing ligands. In fact, we have investigated this in detail in a separate paper (Helliwell & Tanley, 2012) for the case of cisplatin binding to His15 of HEWL after continued X-ray irradiation. In that study, we collected four repeat X-ray diffraction data sets from one crystal; our results show that cisplatin is stable and also that the occupancy values and electron-density maps over the four data sets are the same as the first data set and are comparable to the occupancies presented here and previously (Tanley *et al.*, 2012). Thus, even if radiation damage was the cause of the high $R_{\rm merge}$ values observed here, cisplatin itself is not affected by radiation damage and nor are the occupancy values.

4.3. Cisplatin binding in aqueous conditions

Cisplatin binding to His15 was not observed in aqueous conditions after 4 d of crystal growth. However, X-ray diffraction studies of these crystals after 15 months of prolonged chemical exposure showed cisplatin binding to both binding sites of His15. The occupancy values obtained for both binding sites (N^{δ} = 50% and N^{ε} = 33%) are slightly lower than those obtained for the DMSO conditions. Thus, this system of chemical conditions presumably still has not reached a chemical equilibrium, *i.e.* this is speeded up in the presence of DMSO.

4.4. Stability of cisplatin and carboplatin over prolonged storage

A study by Kristjansson *et al.* (1988) looked at the stability of cisplatin in pharmaceutical formulations and whether cisplatin formed toxic oligomers over a period of one year. Pharmaceutical formulations of cisplatin contain 0.9% NaCl solution. The study by Kristjansson and coworkers determined that the potentially toxic oligomeric products were unstable in NaCl and that solutions of these oligomeric compounds were converted back to cisplatin in NaCl conditions. Our study used a 10% NaCl solution in the crystallization conditions; thus, at this high NaCl concentration cisplatin would be stable and would not form these potentially toxic products.

Carboplatin stability has been studied by Sewell *et al.* (1987) and Gust & Schnurr (1999). The study by Sewell *et al.* (1987) suggested that carboplatin reconstituted in water at a concentration of 10 mg ml^{-1} is stable for 14 d. On the other hand, Gust & Schnurr (1999) tested the stability of carboplatin (1 mg ml^{-1}) in 0.9% NaCl solution; after 28 d of storage at RT they found that 10% of the carboplatin was converted to cisplatin, while only 3% was converted after storage at 277 K for 28 d. The carboplatin crystals used in our study were stored at RT for 13 months and had a 10% NaCl solution added to the crystallization conditions. Hence, it would be expected that most of the carboplatin would be converted to cisplatin after such a prolonged length of storage; however, the binding sites after 13 months prolonged chemical exposure with both cryo and RT data collection show evidence for the CBDC moiety; hence, no conversion is seen in this study. This lack of conversion could be a consequence of the binding of carboplatin to His occurring very quickly in solution and of the formation of crystals within days; hence, the carboplatin was 'captured' in its starting chemical form.

4.5. Impact of these results

The result of cisplatin binding to HEWL in aqueous media after prolonged crystal storage shows that over time cisplatin can bind to HEWL and possibly other proteins which have free histidine residues (Zimmermann & Burda, 2010; Hahn *et al.*, 2001), *i.e.* even in the absence of DMSO. This could be important when considering treatment lengths for patients who are given cisplatin, as over a prolonged

period of time cisplatin will bind to proteins in the body if it is not broken down and expelled before it accumulates.

5. Conclusions

Over a prolonged period of crystallization and chemical exposure (15 months), cisplatin binds to His15 of HEWL in aqueous media, as opposed to a lack of binding after 4 d of crystallization and crystal growth. The use of RT data collection compared with cryocooling and X-ray diffraction data collection at 100 K led to more detail being observed for the CBDC moiety of carboplatin in the N^{ε} binding site electron-density map, thus helping us to discern more detail in the N^{δ} binding site electron-density map for the previous cryocooled data sets (Tanley *et al.*, 2012). Comparing carboplatin binding at the N^{ε} binding site between the 13 months prolonged chemical exposure RT data set, the 8 d crystallization cryocooled data set and the 13 months prolonged chemical exposure cryocooled data set shows that data collection at RT and not the length of the crystallization time causes increased detail in the electron-density map of the ligand to be observed.

Are our results here widely applicable, notably to human proteins and in a medical context? The main point is the chemical one that the interaction of histidine with these two platinum compounds is neatly investigated *via* His15 in HEWL. This is quite generic and we believe that it is indeed, therefore, widely applicable. Of course, the crystallization mixture is chemically specific for HEWL.

JRH is grateful to the University of Manchester for general support, to the ESPRC for a PhD studentship to SWMT and to the School of Chemistry for crystallization, computing and X-ray facilities. We are grateful to Dr Chris Muryn of the School of Chemistry for his stewardship of the APEX II CCD X-ray diffractometer.

References

Arnesano, F. & Natile, G. (2008). *Pure Appl. Chem.* **80**, 2715–2725.
Blow, D. M. (2002). *Acta Cryst.* D**58**, 792–797.
Boal, A. K. & Rosenzweig, A. K. (2009). *J. Am. Chem. Soc.* **131**, 14196–14197.
Calderone, V., Casini, A., Mangani, S., Messori, L. & Orioli, P. L. (2006). *Angew. Chem. Int. Ed. Engl.* **45**, 1267–1269.
Casini, A., Gabbiani, C., Mastrobuoni, G., Messori, L., Moneti, G. & Pieraccini, G. (2006). *ChemMedChem*, **1**, 413–417.
Casini, A., Gabbiani, C., Mastrobuoni, G., Pellicani, R. Z., Intini, F. P., Arnesano, F., Natile, G., Moneti, G., Francese, S. & Messori, L. (2007). *Biochemistry*, **46**, 12220–12230.
Casini, A., Guerri, A., Gabbiani, C. & Messori, L. (2008). *J. Inorg. Biochem.* **102**, 995–1006.
Casini, A., Mastrobuoni, G., Temperini, C., Gabbiani, C., Francese, S., Moneti, G., Supuran, C. T., Scozzafava, A. & Messori, L. (2007). *Chem. Commun.*, 156–158.
Cianci, M., Helliwell, J. R. & Suzuki, A. (2008). *Acta Cryst.* D**64**, 1196–1209.
Crider, S. E., Holbrook, R. J. & Franz, K. J. (2010). *Metallomics*, **2**, 74–83.
Cruickshank, D. W. J. (1999). *Acta Cryst.* D**55**, 583–601.
Emsley, P. & Cowtan, K. (2004). *Acta Cryst.* D**60**, 2126–2132.
Fischer, S. J., Benson, L. M., Fauq, A., Naylor, S. & Windebank, A. J. (2008). *Neurotoxicology*, **29**, 444–452.
Gust, R. & Schnurr, B. (1999). *Monatsh. Chem.* **130**, 637–644.
Hahn, M., Kleine, M. & Sheldrick, W. S. (2001). *J. Biol. Inorg. Chem.* **6**, 556–566.
Hartinger, C. G., Ang, W. H., Casini, A., Messori, L., Keppler, B. K. & Dyson, P. J. (2007). *J. Anal. At. Spectrom.* **22**, 960–967.
Helliwell, J. R. & Tanley, S. W. M. (2012). *Acta Cryst.* D**68**, doi: S090744491204423X.
Huličiak, M., Vacek, J., Sebela, M., Orolinová, E., Znaleziona, J., Havlíková, M. & Kubala, M. (2012). *Biochem. Pharmacol.* **83**, 1507–1513.
Ivanov, A. I., Christodoulou, J., Parkinson, J. A., Barnham, K. J., Tucker, A., Woodrow, J. & Sadler, P. J. (1998). *J. Biol. Chem.* **273**, 14721–14730.
Kristjansson, F., Sternson, L. & Lindenbaum, S. (1988). *Int. J. Pharm.* **41**, 67–74.
McCoy, A. J., Grosse-Kunstleve, R. W., Adams, P. D., Winn, M. D., Storoni, L. C. & Read, R. J. (2007). *J. Appl. Cryst.* **40**, 658–674.
McNicholas, S., Potterton, E., Wilson, K. S. & Noble, M. E. M. (2011). *Acta Cryst.* D**67**, 386–394.
Ramagopal, U. A., Dauter, Z., Thirumuruhan, R., Fedorov, E. & Almo, S. C. (2005). *Acta Cryst.* D**61**, 1289–1298.
Schreurs, A. M. M., Xian, X. & Kroon-Batenburg, L. M. J. (2010). *J. Appl. Cryst.* **43**, 70–82.
Sewell, G. J., Riley, C. M. & Rowland, C. G. (1987). *J. Clin. Pharm. Ther.* **12**, 427–432.
Sheldrick, G. M. (2008). *Acta Cryst.* A**64**, 112–122.
Tanley, S. W. M., Schreurs, A. M. M., Kroon-Batenburg, L. M. J., Meredith, J., Prendergast, R., Walsh, D., Bryant, P., Levy, C. & Helliwell, J. R. (2012). *Acta Cryst.* D**68**, 601–612.
Vagin, A. & Teplyakov, A. (2010). *Acta Cryst.* D**66**, 22–25.
Zimmermann, T. & Burda, J. V. (2010). *Interdiscip. Sci.* **2**, 98–114.